



Effect of powder variability on laser powder bed fusion processing and properties of 316L

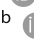



Downloaded from: <https://research.chalmers.se>, 2022-10-11 19:49 UTC

Citation for the original published paper (version of record):

Riabov, D., Cordova Gonzalez, L., Hryha, E. et al (2022). Effect of powder variability on laser powder bed fusion processing and properties of 316L. *European Journal of Materials*, 2(1): 202-221. <http://dx.doi.org/10.1080/26889277.2022.2064772>

N.B. When citing this work, cite the original published paper.

Effect of powder variability on laser powder bed fusion processing and properties of 316L

Dmitri Riabov^{a,b} , Laura Cordova^a , Eduard Hryha^a  and Sven Bengtsson^b 

^aDepartment of Industrial Materials and Science, Chalmers University of Technology, Gothenburg, Sweden; ^bHöganäs AB, Höganäs, Sweden

ABSTRACT

To date, the effects of powder properties, both physical and chemical, on the printed properties of as-built components is still a topic that is poorly understood. A contributing factor is the lack of relevant methods for evaluating the rheological properties of powder, or flowability. This study presents a review of different 316L powder grades that were produced using various atomization techniques. The physical powder properties were evaluated using powder metallurgical techniques, a powder rheometer (FT4) and a rotating drum analyser (RPA). The results indicate that both the FT4 and RPA are suitable for powder characterization. However, the parameter selection for evaluation must be done keeping in mind the application, in this case thin layer powder spreading. It was found that all bulk powder density measurements, basic flow energy and the break energy were able to both differentiate between powder grades and predict how suitable the powder will be for the laser-based powder-bed fusion process. Despite some printability challenges of the water atomized grades at higher layer thicknesses, it was found that both gas atomized grades performed similarly despite minor differences in particle size distribution. Furthermore, powder variability did not show any detrimental effects on the resulting mechanical properties.


ARTICLE HISTORY

Received 1 December 2021
Accepted 7 April 2022

KEYWORDS

Laser-based powder bed fusion (LB-PBF); atomization; flowability; mechanical properties; powder; additive

CONTACT Dmitri Riabov  riabov@chalmers.se  Department of Industrial and Materials Science, Chalmers University of Technology, Rännvägen 2A, Gothenburg SE 41296, Sweden

 Supplemental data for this article can be accessed online at <https://doi.org/10.1080/26889277.2022.2064772>.

© 2022 The Author(s). Published by Informa UK Limited, trading as Taylor & Francis Group.

This is an Open Access article distributed under the terms of the Creative Commons Attribution License (<http://creativecommons.org/licenses/by/4.0/>), which permits unrestricted use, distribution, and reproduction in any medium, provided the original work is properly cited.

Introduction

With the growing industrial application of laser-based powder bed fusion (LB-PBF) there has been an increase in the amount of powder suppliers and powder grades. Despite similar atomizing technologies, the quality of the powder feedstock can vary significantly between suppliers and batches in terms of powder flowability, impurities, and powder surface chemistry. While high-quality powder has its mandated uses, there are instances where high purity is not essential, allowing for lower-cost powder to be considered.

Powder produced by vacuum induction inert gas atomization (VIGA) is considered the industry standard for LB-PBF processes due to its high sphericity, purity, and low oxygen content. The VIGA method offers flexibility hence it can be used for atomization of various material groups (Co, Fe, Ni, Cu-base, etc.). However, the properties of VIGA powder carry a price premium. Therefore, for more cost-sensitive applications alternative powder grades need to be investigated. For example, conventional gas atomized powder, produced using open-air melting and N_2 atomization, or even water atomized grades. Water atomized powder grades have already been shown to work in LB-PBF, both in single-track experiments (Scipioni Bertoli, Guss, Wu, Matthews, & Schoenung, 2017) and in printing bulk components to near full density (Hoeges, Zwiren, & Schade, 2017; Riabov, Hryha, Rashidi, Bengtsson, & Nyborg, 2020; Irrinki et al., 2016). These options are viable for many steels, including tool-steels, and stainless steels but are less suitable for alloys containing reactive elements.

To facilitate the use of alternative powder grades in LB-PBF, the effects of powder properties and powder surface chemistry on printability and resulting mechanical performance must be investigated and understood. Especially connecting the physical powder properties to the spreadability and the printed density during LB-PBF processing. The spreadability is often connected to the flowability of powder; however, both are rheological properties. The terms spreadability and flowability describe the rheological properties under different conditions, e.g., Hall-flowability describes unconfined, free flow while spreadability occurs during more confined conditions.

In powder metallurgy, powder properties are measured by apparent densities (ADs) and tapped densities (TDs), and flowability through a Hall funnel. While these measurement methods are easy to use, repeatable, and accessible, they require free-flowing powder. Hence, limiting their usability for LB-PBF powder, that is, not always free-flowing due to the small particle size. Also, the applicability of Hall-flow to the powder bed fusion processes has often been questioned (Sun et al., 2015;

Schulze, 2007; Lefebvre et al., 2020; Slotwinski & Garboczi, 2015; Cordova, Bor, de Smit, Campos, & Tinga, 2020), as it measures the ability of powder to flow freely rather than its ability to be spread. As a consequence, alternative methods of measuring powder properties are being implemented (Vock, Klöden, Kirchner, Weißgärber, & Kieback, 2019). Namely, the Freeman FT4 and various rotating drum analysers (RPAs) have seen increasing use within the powder bed community as they extend the measurement capabilities (Lefebvre et al., 2020; Marchetti & Hulme-Smith, 2021; Mussatto et al., 2021). The use of these methods does not however provide an obfuscating image of what can be considered a *well-performing* powder for LB-PBF. This is due to the many parameters that both methods produce and the difficulty of interlinking these to spreadability and the overall printing performance.

Several studies have used one of these methods to characterize powder for LB-PBF, showing that non-flowing powder can be measured and that the methods are capable of distinguishing between powder batches, virgin and reused powder, etc. (Spierings, Voegtlin, Bauer, & Wegener, 2016; Pleass & Jothi, 2018; Espiritu, Kumar, Nommeots-Nomm, Lerma, & Brochu, 2020; Strondl, Lyckfeldt, Brodin, & Ackelid, 2015; Mellin et al., 2017; Sutton, Kriewall, Karnati, Leu, & Newkirk, 2020; Yablokova et al., 2015; Haferkamp et al., 2021). Yet, there are few studies that provide a holistic view of the powder properties and linking them to a measure of printability, which can be defined according to how well a powder grade is able to be consolidated to near full density. Of the few studies, one by Seyda, Herzog, and Emmelmann (2017) looked at the flowability and printability of three different Ti-6Al-4V alloy powder grades. The study used both the FT4 and RPA to analyse the powder. Yet, the powder with the lowest measured flowability printed to the highest densities. A similar study was performed by Brika, Letenneur, Dion, and Brailovski (2020) where, in addition to the powder flowability evaluations, the powder bed density was analysed. It was found that the powder bed density correlated with the flowability and also the printed density.

Therefore, this study aims to bridge that gap by looking at different powder grades, their physical and chemical properties and interlinking these with a measure of how well these grades print in an LB-PBF machine. This measure would include the concepts of spreadability and the ability to reach high densities without large defects.

Experimental

Three different commercially available 316L powder grades were provided by Höganäs AB. The VIGA powder was supplied in the sieve fraction

of 15–45 μm , while the remaining grades were supplied in the sieve fraction 25–53 μm . The WA powder was also modified using a mechanical treatment to study whether the powder properties could be improved, this grade was denoted *WA-M*. The chemical compositions were acquired using various techniques, namely inductively coupled plasma optical emission spectroscopy (SPECTRO ARCOS) for majority of the elements together with combustion and hot fusion gas analysis (LECO ON836 and CS836) for the analysis of C, O, N, and S.

Powder surfaces were analysed in the as-received state using x-ray photoelectron spectroscopy (XPS) where a PHI 5500 was utilized. The instrument was equipped with a monochromatic Al K_{α} source with a beam size of 0.8 mm hence analysing large number of particles simultaneously. The generated photoelectrons were collected in a hemispherical analyser at a pass energy of 93.9 eV with a step size of 0.4 eV.

Overview images of the powder grades were taken using a scanning electron microscope (SEM) at an accelerating voltage of 15 kV (Philips XL 30). SEM was also used to view the fracture surfaces; however, for this purpose a Leo Gemini 1550 operating at 1 kV was used instead.

The physical powder properties such as Hall-flow, AD, and TD were measured according to ISO 4490:2018, 3923-1:2018, and 3953:2011 (three replicates per test), respectively. The particle size distribution was measured with laser diffraction (Sympatec HELOS). Additional properties were measured using the Freeman FT4, where two stability and rate sensitivity tests per powder grade were run. Lastly, the powder grades were measured using a Revolution Powder Analyser (RPA), by Mercury Scientific, running both flowability (with constant RPM of 0.6) and multiflow (RPM is ramped up to 70) test. During these tests, 25 ml of untapped powder was used, and each test was repeated three times. In LB-PBF, the re-coater speed ranges from 50 to 200 mm/s, hence relevant RPMs for LB-PBF range from 10 to 40 RPM. The settings and explanation of the parameters of FT4 and RPA are given in more detail in the Supplemental Material.

Samples in the form of cylinders with a diameter of 10 mm, tensile test bars (see Figure 1) and notched impact toughness bars were built in an EOS M290 machine. The cylinders were built using varying layer thicknesses of 20, 40, 60, and 80 μm . Three cylinders per powder grade and layer thickness were printed. The standard EOS parameters were used for 20 and 40 μm , 316L_SurfaceM291 1.10 and 316L_040_FlexM291 1.00, respectively. While for 60 and 80 μm the parameters were developed in-house, all parameters are summarized in Table 1. Contouring was used for 20 and 40 μm layer thicknesses. Specimens for the mechanical evaluation were produced with a layer thickness of 20 μm using standard EOS parameters, as this setting produced comparable porosity levels.

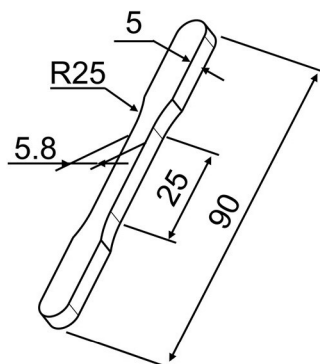


Figure 1. Geometry of the tensile test specimens, in mm.

Table 1. The utilized bulk parameters when printing with 20, 40, 60, and 80 μm layer thickness settings.

| | 20 μm | 40 μm | 60 μm | 80 μm |
|--|------------------|------------------|------------------|------------------|
| Laser power (W) | 195 | 214 | 220 | 220 |
| Scan speed (mm/s) | 1083 | 928 | 900 | 800 |
| Hatch distance (mm) | 0.09 | 0.1 | 0.09 | 0.09 |
| Volumetric energy density (J/mm^3) | 100 | 58 | 45 | 38 |

Contouring was used for 20 and 40 μm layer thicknesses. Prior to each build the chamber was flushed with argon gas of purity 5.0 and oxygen content was kept at 0.1% throughout the build, sufficient flow was maintained by a differential turbine pressure of 0.56 bar. Re-coater speed was at the default value of 80 mm/s, corresponding to 15 RPM in the RPA. Sample geometries were built to near net shape.

The residual porosity of the cylinders was evaluated using light optical microscopy (LOM), Zeiss Axioscope 7 (Oberkochen, Germany). Cross-sections were prepared by sectioning and mounting in Bakelite. The samples were then plane ground using 220# grit SiC paper, fine ground using 9 μm diamond suspension and finally polished using napped cloths using 3 and 1 μm diamond suspensions. Images of the cross sections were stitched together using Zeiss software (Axiovision) and analysed using the software imageJ.

Finally, the tensile properties were evaluated in as-built condition using a Zwick Z100 test machine according to ISO 6892-1 (three samples per powder grade) and impact toughness was evaluated using a pendulum impact tester by Instron Wolpert (seven samples per powder grade). A summary of the experimental plan is given below in Table 2. Statistical analysis, *t*-tests, and one-way ANOVA, of the results was performed using the software JMP Pro version 15 (Marlow, UK).

Table 2. Summary of the experimental procedure, outlining what experiments were performed with which powder grade.

| | VIGA | GA | WA | WA-M |
|---------------------------------|------|----|----|------|
| XPS | ✓ | ✓ | ✓ | |
| Conventional powder flowability | ✓ | ✓ | ✓ | ✓ |
| FT4 and RPA | ✓ | ✓ | ✓ | ✓ |
| Printing M290 | ✓ | ✓ | ✓ | ✓ |
| Mechanical properties | ✓ | ✓ | ✓ | |
| Fractography | ✓ | ✓ | ✓ | |

Results

Powder properties

Figure 2 displays SEM images of the studied powder grades. Both the VIGA and GA powder showed typical spherical morphology of gas atomized powder. The surfaces of the VIGA and GA did not have any large visible oxides, and presence of satellites was minimal. The WA powder had typical irregular morphology of a water atomized powder. The modification of WA was clearly seen in the micrograph of the WA-M grade, as the particles appeared more spherical with most of the irregularities smoothed out.

The results from the chemical evaluations are presented in Table 3. The composition of WA-M was the same as WA. All the grades showed rather similar composition, the VIGA powder having slightly higher contents of both Cr and Ni. Other differences that were significant were the lower Mn content of the WA powder accompanied by the higher oxygen content. Additionally, due to the N₂ gas atomization, the GA powder showed some nitrogen pick-up.

The XPS survey scans as seen in Figure 3 showed that the as-received surfaces were predominantly covered by oxide-forming elements Fe, Cr, Mn, and Si. Looking solely at the spectra, the two gases atomized grades show many resemblances in terms of visible peaks and peak locations with one exception; there was no Si detected on the VIGA powder. The WA powder had some more pronounced differences. Mn was not detected on the surface, intensity of the Si peak was higher, and peaks of Fe, C, and O were shifted slightly to higher energy values. A more detailed analysis of the powder surface chemistry can be found elsewhere (Riabov, Hryha, et al., 2020).

Table 4 presents the physical properties of the powder using the conventional PM techniques. Additionally, the particle size distribution as measured by laser diffraction is also provided. As observed below, the two gas atomized grades have similar AD and TD while the VIGA

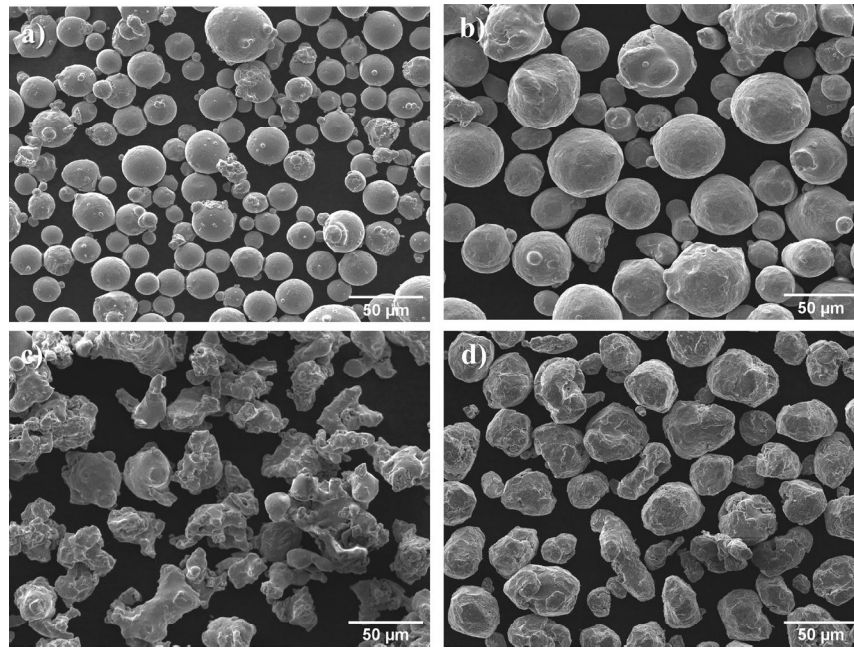


Figure 2. SEM images of the studied powder grades, a) VIGA, b) GA, c) WA, and d) WA-M.

Table 3. Chemical compositions in weight percent of the studied powder grades.

| Powder | C | O | N | S | Si | Cr | Ni | Mn | Mo | P | Fe |
|--------|------|------|------|-------|------|------|------|------|-----|-------|------|
| VIGA | 0.01 | 0.03 | 0.02 | 0.005 | 0.05 | 18.0 | 14.2 | 1.4 | 2.9 | 0.004 | Bal. |
| GA | 0.01 | 0.07 | 0.14 | 0.007 | 0.7 | 16.5 | 12.3 | 1.5 | 2.5 | 0.02 | Bal. |
| WA | 0.03 | 0.24 | 0.04 | 0.005 | 0.8 | 16.9 | 12.7 | 0.17 | 2.2 | 0.02 | Bal. |

powder had somewhat faster flow through the Hall-flow funnel at 15.9 s. The WA powder, however, had both lower flowability and powder density values as compared to the GA and VIGA powder. This is usually attributed to the powder morphology, causing the individual particles to interlock hence lowering their ability to flow and densely arrange. Modification of the WA grade resulted in a significant improvement of both, flowability and density values, to an extent where it was comparable with the gas atomized grades. In short, it was possible to clearly differentiate the WA grade from the others, while the gas atomized powder measured similarly.

The results of the measurements using the FT4 are presented below in Figure 4 where two flowability tests per powder were ran. The presented properties are basic flow energy (BFE), specific energy (SE), and the measured bulk density. Like the values presented in Table 4, a clear

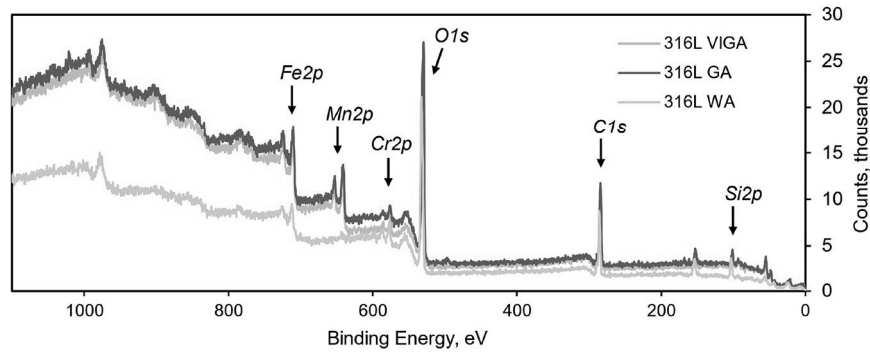


Figure 3. XPS survey scans of the studied powder grades.

Table 4. Physical properties of the tested powder grades.

| Grade | AD (g/cm ³) | TD (g/cm ³) | Flow (s/50 g) | x ₁₀ (μm) | x ₅₀ (μm) | x ₉₀ (μm) |
|-------|-------------------------|-------------------------|---------------|----------------------|----------------------|----------------------|
| VIGA | 4.4 ± 0.01 | 5.1 ± 0.03 | 15.9 ± 0.1 | 18.1 | 31.1 | 52.0 |
| GA | 4.3 ± 0.01 | 4.9 ± 0.04 | 18.1 ± 0.3 | 26.1 | 42.2 | 63.3 |
| WA | 2.4 ± 0.01 | 3.1 ± 0.02 | 37.4 ± 0.6 | 25.8 | 46.5 | 70.4 |
| WA-M | 3.7 ± 0.03 | 4.6 ± 0.02 | 16.4 ± 0.1 | 24.9 | 41.0 | 58.8 |

differentiation can be seen between the WA and the two gas atomized powder grades. The WA-M grade was shown to perform better than the WA powder but worse than the two gas atomized powder grades. The differences between VIGA and GA were less apparent, at least during the first eight tests that are conducted with the same blade RPM. Tests made with slower RPM (test 9–11) showed some differences between VIGA and GA, where the VIGA powder displayed higher energy values hence providing higher resistance to the blade. WA did not seem to be affected by the change in RPM. Figure 4(b) displays in addition to the BFE also average SE and bulk density values. Some minor differences relative to the values in Table 4 appeared between VIGA and GA, where GA had marginally higher bulk density than VIGA.

Figure 5 presents the results from the RPA measurements with the following properties: avalanche energy (AE), break energy (BE), avalanche angle (AA), and the dynamic density. A summary of the mean values and standard deviations can be found in Table A1 (Appendix). The AE, BE, and AA were evaluated using two different measurements, a flowability test that evaluates avalanches at a constant RPM of 0.6 and a multiflow test where the avalanching behaviour was investigated as a function of increasing RPM. The results of the flowability tests are presented in Figure 5(a, c, and e), where a distribution of all of the recorded avalanches is seen. Previous testing showed clear differentiation

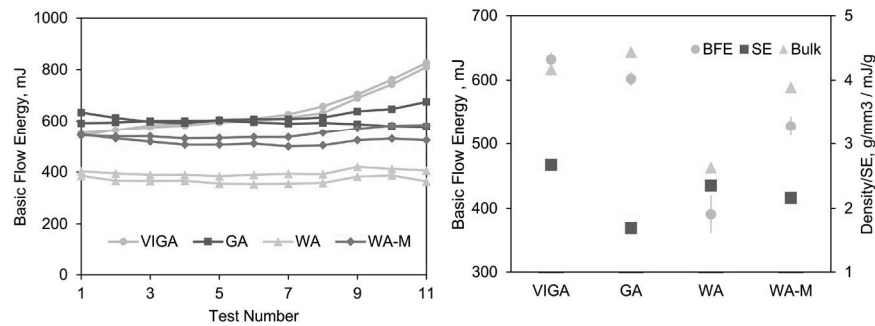


Figure 4. Results from powder measurements using the FT4. a) Stability and rate sensitivity tests, b) summary of measured BFE, SE, and Bulk density properties (standard deviations were in many cases smaller than the figure symbols).

between WA and the gas atomized grades, with WA-M performing in-between the two. The sole RPA property that correlated with the previous findings was BE. The BE values of WA were both higher and had a larger spread between avalanches with the lowest and highest recorded BE. The other energy descriptor, AE, did not correlate with the previous measurements and showed that GA and VIGA had the highest and lowest AE, respectively. Lastly, the AA differentiated GA from VIGA, and WA from the two other gas atomized grades.

The multiflow tests are presented in Figure 5(b, d, f, and g). Increasing the RPM led to more erratic AE results although the shape of the curves of the different grades was similar except for WA. The avalanching behaviour was probably undergoing changes in the 10–30 RPM regime, from slumping to rolling or even cascading. This could provide an explanation to the erratic results. The BE parameter was found to show similar trend as in the flowability test, but with the WA-M grade approaching WA at higher RPMs. The AA during the multiflow tests remained similar to what was shown during the flowability test, but the slope of the WA grade was less steep; indicating that the AA of the WA grade is less sensitive to the RPM. Additionally, a statistical analysis was performed to check significance of the difference between VIGA and GA powder grades, which can be found in Table A2 (Appendix). The density values remained relatively constant up to 40 RPM, at higher speeds the powder was aerated more hence the density values started decreasing.

Finally, a comparison between the AD and the bulk densities as measured by the FT4 and RPA is shown in Figure 6. Both methods showed good correlation to the AD and hence can be used to measure bulk densities of non-flowing powder.

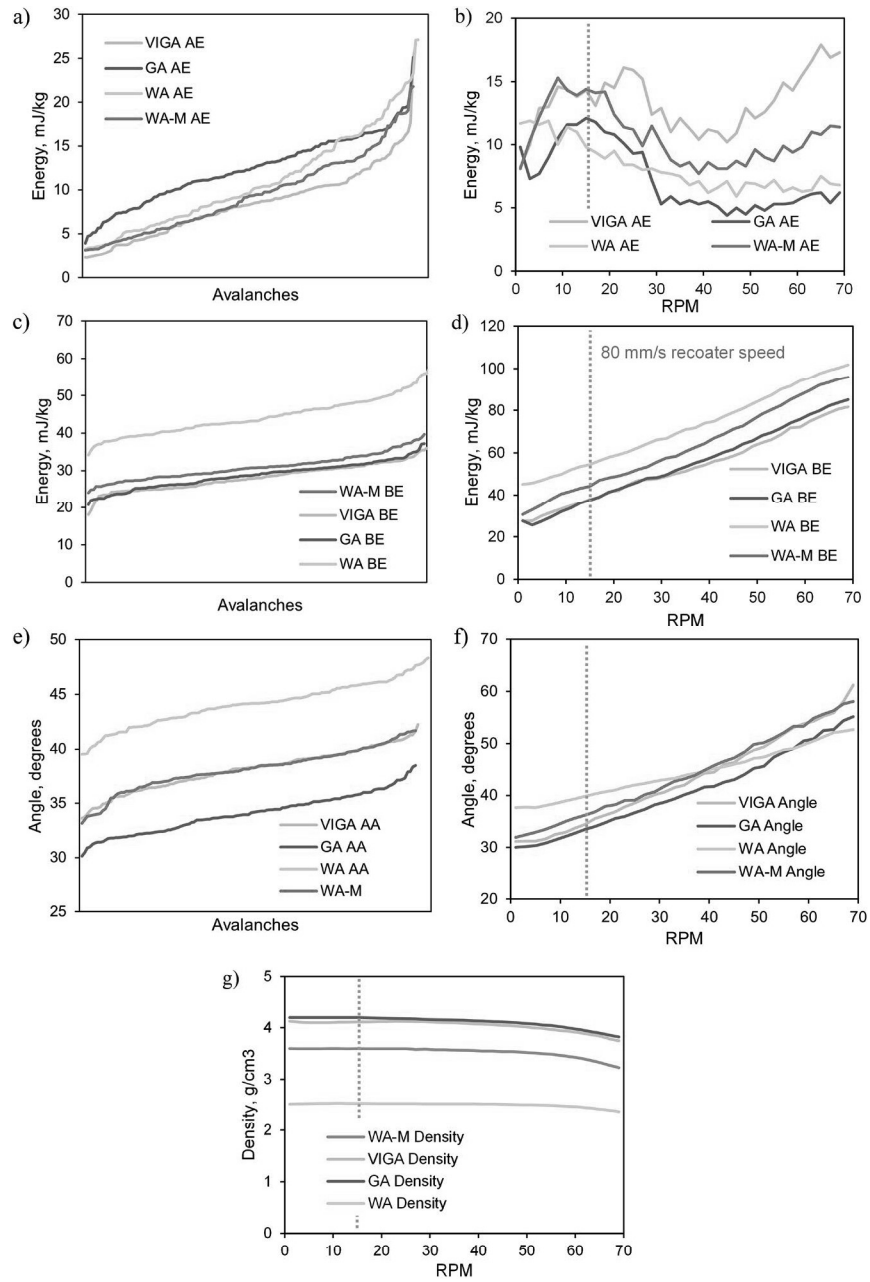


Figure 5. Results from powder measurements using the RPA. a,b) Flowability and multiflow tests evaluating the AE. c,d) Flowability and multiflow tests evaluating the BE. e,f) Flowability and multiflow tests evaluating the AA. g) Multiflow test evaluating the dynamic density.

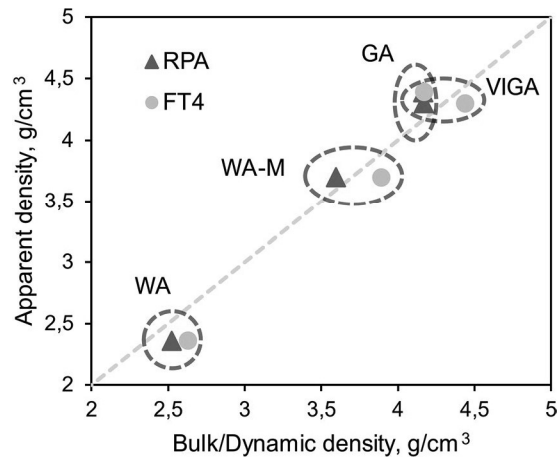


Figure 6. Comparison of bulk measurements using FT4 and RPA relative to the apparent density (y-axis). A dashed line with the slope of 1 was added to provide ease of viewing.

As-printed properties

All powder grades were processed by an EOS M290 machine using various layer thicknesses, from 20 to 80 μm , with the resulting porosity presented below in Figure 7. At 20 μm layer thickness the difference in printability was not significant (see Table A3 in the Appendix), with all the investigated samples having a residual porosity of <0.05%. At layer thicknesses of 40 μm and above the residual porosity in samples printed using WA powder rapidly increased up to several percent. The WA-M grade showed a similar trend, although at a lower rate. Hence, printability was increased by modifying the powder. However, samples printed using GA and VIGA powder grades continued to have low residual porosity up to 80 μm when using the same process parameters. At 80 μm , it appeared as if the VIGA powder printed to somewhat higher densities as compared to the GA powder.

The mechanical properties of samples built using the investigated powder grades are presented in Figure 8. The samples produced using GA powder were the strongest; however, the highest elongation to fracture was attained by samples built using VIGA powder. Since samples for mechanical testing were printed using a 20 μm layer thickness, the porosity within the samples was comparable. Therefore, the small compositional differences were most likely responsible for the strength response. Impact toughness values were similar between VIGA and GA samples while the WA produced significantly lower values.

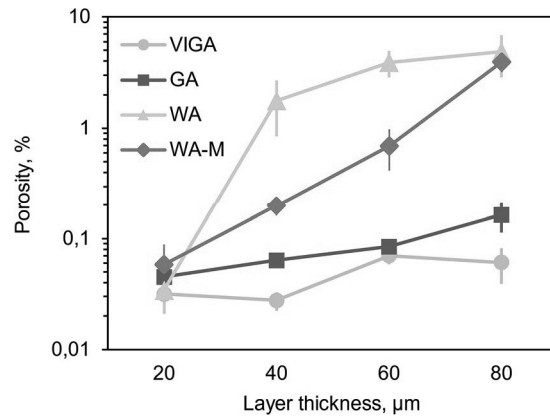


Figure 7. Results of the porosity as a function of the layer thickness, note the logarithmic scale on the y-axis.

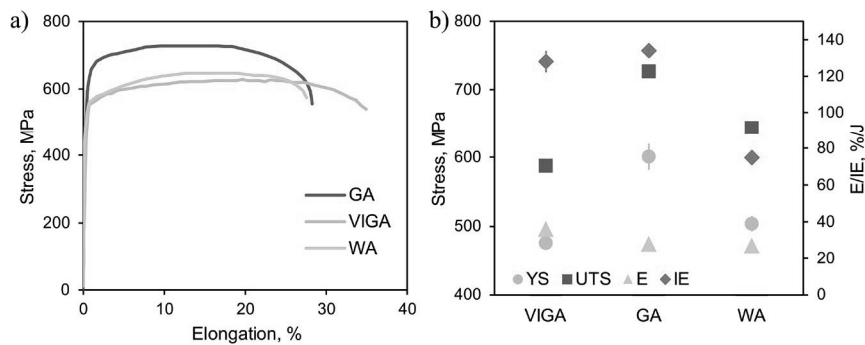


Figure 8. Results of a) tensile tests of printed components using VIGA, GA, and WA powder. b) Summary of the mechanical testing, elongation, and impact toughness are shown on the right y-axis (the standard deviation is in many cases smaller than the figure symbols).

Fractography of the impact toughness samples revealed similar features between all tested powder grades with no significant differences between the samples, as can be seen in Figure 9. The fracture mode was ductile with fine dimples. Small oxide inclusions could often be seen at the bottom of the dimples. The dimple size was not found to vary greatly between the different powder grades.

Discussion

To provide an ease of reference the different physical powder properties were summarized below in Table 5. The powder grades are ranked

according to their performance and labelled *low*, *medium*, or *high*. The performance can be considered high if a powder reaches high densities or flows fast through the Hall-flow funnel. For the RPA parameters, low AE, BE, and AA will be considered as high performing. For the FT4 parameters, high BFE will be considered high performance, while high SE will be considered low.

The initial SEM images of the powder clearly showed morphological differences between the gas atomized grades and the WA powder. The morphology impacts most of the physical properties, where the highly irregular shape of WA particles limits free-flow. The individual particles inter-lock with each other and hinder efficient particle arrangement, resulting in low ADs and TDs, and low flowability during Hall-flow experiments. These differences were also noticeable with the results of the FT4 and some of the results produced by RPA.

As mentioned, many of the physical characterization methods can clearly differentiate between the WA grade and the gas atomized grades (GA and VIGA). The FT4 parameter that reflected this is the BFE and it was found to decrease as the AD/TD of the powder decreased. This is not surprising, as a denser powder bed will provide more resistance to the blade as it plunges down. On the upstroke of the blade, only the amount of powder (or density as powder volume is kept constant) and its cohesiveness should influence the resistance. However, the VIGA powder did not follow this trend and instead displayed higher values relative to the GA grade. This behaviour can be related to the finer particle size of the VIGA powder that will have a higher surface area, increasing the drag force during the upstroke movement.

The RPA was able to differentiate between most of the investigated powder grades, but the different parameters strongly depended on the rotation speed. Earlier research has indicated that low AA and AE values can be indicative of a well-flowing powder (Fu et al., 2011; Krantz, Zhang, & Zhu, 2009; Amado, Schmid, & Wegener, 2014; Nalluri & Kuentz, 2010; Goh, Heng, & Liew, 2018). Yet, we could not find such indications in this study that were consistent through both flowability and multiflow testing. The erratic behaviour of AE during the multiflow testing can be on the one hand explained by avalanching regimes with different Froude numbers (Mellmann, 2001). On the other hand, both BE and AA showed consistent increases with the RPM despite also going through different avalanching regimes, suggesting that the algorithm for calculating AE might be unstable at higher RPMs. Both the BE and the bulk density were found to correlate closely with the previous findings, both during constant and variable RPM testing. This is in good agreement with Trpělková, Hurychová, Kuentz, Vraníková, and Šklubalová (2020) who showed that BE correlates well with powder cohesion, hence providing

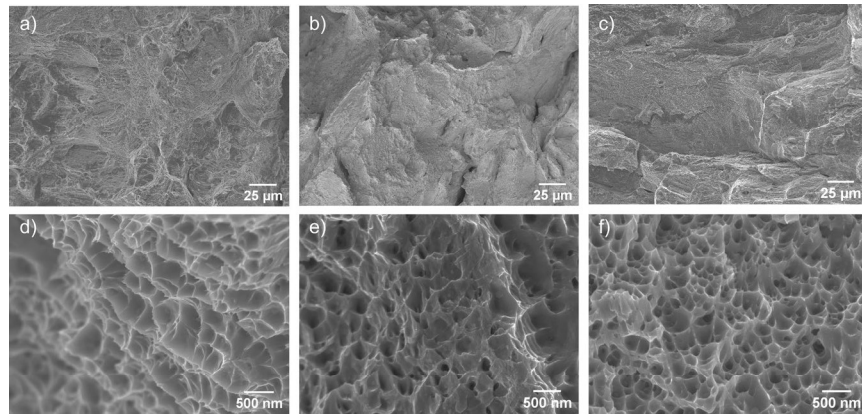


Figure 9. SEM images of fracture surfaces from impact energy specimens. a) VIGA, b) GA, and c) WA. d–f) high magnification images showing the dimples.

Table 5. Performance indicator of the measured physical powder properties.

| Powder grade | Traditional | | | FT4 | | | RPA | | | |
|--------------|-------------|------|-----------|------|------|------|------|------|------|---------|
| | AD | TD | Hall-flow | BFE | SE | Bulk | AE | BE | AA | Density |
| VIGA | High | High | High | High | Med | High | High | High | Med | High |
| GA | High | High | High | High | High | High | Low | High | High | High |
| WA | Low | Low | Low | Low | Med | Low | High | Low | Low | Low |
| WA-M | Med | High | High | Med | Med | Med | High | Med | Med | Med |

a sensitive parameter suitable for characterization of powder flowability. Similar to the FT4, the RPA was able to show that the WA-M grade performed somewhere in between the WA and the gas atomized grades; contrary to the results of the Hall-flow experiments that showed similar performance between WA-M, VIGA, and GA. This explains the sensitivity of different characterization techniques.

Comparing the measurement methods to the suitability for powder characterization for LB-PBF is not easy. The traditional measurement methods such as Hall-flow and AD have their merit. They are accessible, easy to use, and interpretation of the results is straight forward. However, it was also shown that Hall-flow can sometimes be misleading, as seen in the WA-M grade. The advantage of the FT4 and the RPA is that they can measure the powder under dynamic conditions, which better represents the LB-PBF process. Although, as seen in this study, the results generated by the FT4 and RPA can be difficult to interpret and must be studied further to fully understand the underlying mechanisms. In addition, the measurement results strongly rely on handling (e.g., cleaning, pouring the powder, etc.) which was found especially true for the FT4. Similar sensitivity of the FT4 to handling was reported by Lefebvre et al.

(2020) in a round-robin study of Ti-6Al-4V powder. Despite this, both the FT4 and RPA were found to provide parameters that correlate to the printability better than the Hall-flowmeter.

Connecting the physical powder properties with printability was also proven to be challenging. In particular, finding relevant powder parameters to assess, and which of these will have a deterministic role in defining printability. The printing process is complex, and it can be expected that a single entity can hardly predict how well a powder grade might perform within the LB-PBF process. Rather, it seems there is an interplay of flowability (e.g., Hall-flow, BFE, or BE) and the powder bed density (e.g., AD or bulk densities). This was highlighted when printing with the WA-M grade. The increase in the performance of the WA-M powder compared to the WA powder shows the importance of the particle morphology for the flowability of the powder. However, despite the morphological change the BFE, BE, and density values were still lower as compared to the gas atomized grades. Resulting in a considerably lower printability as compared to the gas atomized grades, especially at higher layer thicknesses.

It was found that a powder performs well once both powder density and flowability reach a certain threshold, after which other aspects start being more dominant. These other aspects may be the printing parameters, where each powder might have its own optimum. This was shown by Reijonen et al. (2021) in cross-testing of LB-PBF machines and vendor-supplied powder, where finer SLM-supplied powder gave rise to lower porosity relative to an EOS powder when printed with equal parameters. It is also possible that finer powder fills potential perturbations formed on a printed surface better, especially when building using 80 μm layer thicknesses. This would in turn create a closer coupling between the newly spread powder layer and the freshly melted surface layer. However, investigating these aspects was outside the scope of this study.

While the printing trials revealed some limitations of using WA powder grades, the resulting mechanical properties showed that alternative grades are not necessarily weaker or worse. On the contrary, samples produced using both GA and WA powder exhibited higher static strength. Even impact toughness values, that are known for being sensitive to oxygen content within parts, showed higher values in samples built using GA, which is believed to be attributed to its higher strength.

Conclusions

This work examined the effects of powder variability on the processability of 316L stainless steel powder by the LB-PBF process and the resulting mechanical properties. For this purpose, three different powder grades, produced using various atomization techniques, were investigated and

characterized. The physical powder properties were evaluated using various techniques, incorporating both traditional ways of assessing flowability and newly developed commercial equipment. These properties were then connected to the printed densities of specimens produced using the investigated powder grades. The results showed that all powder grades were able to reach high densities when printed. However, significant differences between some powder grades were noted when utilizing layer thicknesses above 20 μm . The main conclusions are as follows:

- All powder grades can print to a density of $\geq 99.5\%$ when printing with a layer thickness of 20 μm .
- Regarding the physical, surface chemistry, and printed properties both the VIGA and GA grades performed similarly.
- The FT4 and RPA managed to differentiate the powder grades according to their printability better than Hall-flow indicated.
- The most significant parameters that were found to correlate with printability were: AD and bulk densities (measured by all methods), BFE (FT4), and BE (RPA).
- High printability is achieved if a powder has both relatively high bulk density ($>4\text{g/cm}^3$) and good flowability ($>550\text{mJ}$ in BFE or $<40\text{mJ/kg}$ in break energy).
- Despite differences in the printability, the mechanical properties were found to be comparable between the powder grades.

Disclosure statement

The authors report there are no competing interests to declare.

Funding

This work has been conducted in the framework of the Centre for Additive Manufacturing – Metal (CAM²), supported by the Swedish Governmental Agency of Innovation Systems (Vinnova).

Notes on contributor





Dmitri Riabov is an industrial PhD student from Höganäs AB. He is part of a research group in powder and surface technology, lead by professor Lars Nyborg, focusing on powder properties for AM and microstructural characterization of AM built stainless steels.

Laura Cordova is a researcher in the group of Powder Metallurgy and Additive Manufacturing, focused on powder life cycle for Additive Manufacturing (AM) processes: from powder production, efficiency of powder utilization during AM, powder rheological characterization, and material recycling.

Eduard Hryha is professor in powder metallurgy and metal additive manufacturing. He is also director of CAM2 competence center focusing on powder-based metal additive manufacturing. His research spans from surface analysis to the relationship between powder and AM processing.

Sven Bengtsson is employed by Höganäs AB as a senior researcher in powder and alloy development for powder-based metal additive manufacturing.

ORCID

Dmitri Riabov  <http://orcid.org/0000-0003-3179-6403>
Laura Cordova  <http://orcid.org/0000-0001-6982-4516>
Eduard Hryha  <http://orcid.org/0000-0002-4579-1710>
Sven Bengtsson  <http://orcid.org/0000-0002-1397-8599>

References

- Amado, A., Schmid, M., & Wegener, K. (2014). *Flowability of SLS powders at elevated temperature*. Zürich, Switzerland: ETH Zurich. Retrieved from <https://doi.org/10.3929/ethz-a-010057815>.
- Brika, S. E., Letenneur, M., Dion, C. A., & Brailovski, V. (2020). Influence of particle morphology and size distribution on the powder flowability and laser powder bed fusion manufacturability of Ti-6Al-4V alloy. *Additive Manufacturing*, 31, 100929. Retrieved from <https://doi.org/10.1016/j.addma.2019.100929>.
- Cordova, L., Bor, T., de Smit, M., Campos, M., & Tinga, T. (2020). Measuring the spreadability of pre-treated and moisturized powders for laser powder bed fusion. *Additive Manufacturing*, 32, 101082. Retrieved from <https://doi.org/10.1016/j.addma.2020.101082>.
- Espiritu, E. R. L., Kumar, A., Nommeots-Nomm, A., Lerma, J. A. M., & Brochu, M. (2020). Investigation of the rotating drum technique to characterise powder flow in controlled and low pressure environments. *Powder Technology*, 366, 925–937. Retrieved from <https://doi.org/10.1016/j.powtec.2020.03.029>.
- Fu, J., Krantz, M., Zhang, H., Zhu, J., Kuo, H., Wang, Y. M., & Lis, K. (2011). Investigation of the recyclability of powder coatings. *Powder Technology*, 211(1), 38–45. Retrieved from <https://doi.org/10.1016/j.powtec.2011.03.016>.
- Yablokova, G., Speirs, M., Van Humbeeck, J., Kruth, J. P., Schrooten, J., Cloots, R. ... Luyten. (2015). Rheological behavior of β -Ti and NiTi powders produced by atomization for SLM production of open porous orthopedic implants. *Powder Technology*, 283, 199–209. Retrieved from <https://doi.org/10.1016/j.powtec.2015.05.015>.
- Goh, H. P., Heng, P. W. S., & Liew, C. V. (2018). Comparative evaluation of powder flow parameters with reference to particle size and shape. *International Journal of Pharmaceutics*, 547(1–2), 133–141. Retrieved from <https://doi.org/10.1016/j.ijpharm.2018.05.059>.
- Irrinki, H., Dexter, M., Barmore, B., Enneti, R., Pasebani, S., Badwe, S. ... Atre. (2016). Effects of powder attributes and laser powder bed fusion (L-PBF) process conditions on the densification and mechanical properties of 17-4 PH stainless steel. *Jom Journal of the Minerals Metals and Materials Society*, 68(3), 860–868. Retrieved from <https://doi.org/10.1007/s11837-015-1770-4>.

- Haferkamp, L., Spierings, A., Rusch, M., Jermann, D., Spurek, M. A., & Wegener, K. (2021). Effect of Particle size of monomodal 316L powder on powder layer density in powder bed fusion. *Progress in Additive Manufacturing*, 6(3), 367–374. Retrieved from <https://doi.org/10.1007/s40964-020-00152-4>.
- Hoeges, S., Zwiren, A., & Schade, C. (2017). Additive manufacturing using water atomized steel powders. *Metal Powder Report*, 72(2), 111–117. Retrieved from <https://doi.org/10.1016/j.mprp.2017.01.004>.
- Krantz, M., Zhang, H., & Zhu, J. (2009). Characterization of powder flow: Static and dynamic testing. *Powder Technology*, 194(3), 239–245. Retrieved from <https://doi.org/10.1016/j.powtec.2009.05.001>.
- Lefebvre, L. P., Whiting, J., Nijikovsky, B., Brika, S. E., Fayazfar, H., & Lyckfeldt, O. (2020). Assessing the robustness of powder rheology and permeability measurements. *Additive Manufacturing*, 35, 101203. Retrieved from <https://doi.org/10.1016/j.addma.2020.101203>.
- Marchetti, L., & Hulme-Smith, C. (2021). Flowability of steel and tool steel powders: A comparison between testing methods. *Powder Technology*, 384, 402–413. Retrieved from <https://doi.org/10.1016/j.powtec.2021.01.074>.
- Mellin, P., Lyckfeldt, O., Harlin, P., Brodin, H., Blom, H., & Strondl, A. (2017). Evaluating flowability of additive manufacturing powders, using the Gustavsson flow meter. *Metal Powder Report*, 72(5), 322–326. Retrieved from <https://doi.org/10.1016/j.mprp.2017.06.003>.
- Mellmann, J. (2001). The transverse motion of solids in rotating cylinders—forms of motion and transition behavior. *Powder Technology*, 118(3), 251–270. Retrieved from [https://doi.org/10.1016/S0032-5910\(00\)00402-2](https://doi.org/10.1016/S0032-5910(00)00402-2).
- Mussatto, A., Groarke, R., O'Neill, A., Obeidi, M. A., Delaure, Y., & Brabazon, D. (2021). Influences of powder morphology and spreading parameters on the powder bed topography uniformity in powder bed fusion metal additive manufacturing. *Additive Manufacturing*, 38, 101807. Retrieved from <https://doi.org/10.1016/j.addma.2020.101807>.
- Nalluri, V. R., & Kuentz, M. (2010). Flowability characterisation of drug-excipient blends using a novel powder avalanching method. *European Journal of Pharmaceutics and Biopharmaceutics*, 74(2), 388–396. Retrieved from <https://doi.org/10.1016/j.ejpb.2009.09.010>.
- Pleass, C., & Jothi, S. (2018). Influence of powder characteristics and additive manufacturing process parameters on the microstructure and mechanical behaviour of Inconel 625 fabricated by Selective Laser Melting. *Additive Manufacturing*, 24, 419–431. Retrieved from <https://doi.org/10.1016/j.addma.2018.09.023>.
- Reijonen, J., Björkstrand, R., Riipinen, T., Que, Z., Metsä-Kortelainen, S., & Salmi, M. (2021). Cross-testing laser powder bed fusion production machines and powders: Variability in mechanical properties of heat-treated 316L stainless steel. *Materials & Design*, 204, 109684. Retrieved from <https://doi.org/10.1016/j.matdes.2021.109684>.
- Riabov, D., Hryha, E., Rashidi, M., Bengtsson, S., & Nyborg, L. (2020). Effect of atomization on surface oxide composition in 316L stainless steel powders for additive manufacturing. *Surface and Interface Analysis*, 52(11), 694–706. Retrieved from <https://doi.org/10.1002/sia.6846>.
- Riabov, D., Rashidi, M., Hryha, E., & Bengtsson, S. (2020). Effect of the powder feedstock on the oxide dispersion strengthening of 316L stainless steel pro-

- duced by laser powder bed fusion. *Materials Characterization*, 169, 110582. Retrieved from <https://doi.org/10.1016/j.matchar.2020.110582>.
- Schulze, D. (2007). *Powders and Bulk Solids*. Berlin, Heidelberg, Germany: Springer Berlin Heidelberg. Retrieved from <https://doi.org/10.1007/978-3-540-73768-1>
- Scipioni Bertoli, U., Guss, G., Wu, S., Matthews, M. J., & Schoenung, J. M. (2017). In-situ characterization of laser-powder interaction and cooling rates through high-speed imaging of powder bed fusion additive manufacturing. *Materials & Design*, 135, 385–396. Retrieved from <https://doi.org/10.1016/j.matdes.2017.09.044>.
- Seyda, V., Herzog, D., & Emmelmann, C. (2017). Relationship between powder characteristics and part properties in laser beam melting of Ti–6Al–4V, and implications on quality. *Journal of Laser Applications*, 29(2), 022311. Retrieved from <https://doi.org/10.2351/1.4983240>.
- Slotwinski, J. A., & Garboczi, E. J. (2015). Metrology needs for metal additive manufacturing powders. *Jom Journal of the Minerals Metals and Materials Society*, 67(3), 538–543. Retrieved from <https://doi.org/10.1007/s11837-014-1290-7>.
- Spierings, A. B., Voegtlin, M., Bauer, T., & Wegener, K. (2016). Powder flowability characterisation methodology for powder-bed-based metal additive manufacturing. *Progress in Additive Manufacturing*, 1(1–2), 9–20. <https://doi.org/10.1007/s40964-015-0001-4>.
- Strondl, A., Lyckfeldt, O., Brodin, H., & Ackelid, U. (2015). Characterization and control of powder properties for additive manufacturing. *Jom Journal of the Minerals Metals and Materials Society*, 67(3), 549–554. Retrieved from <https://doi.org/10.1007/s11837-015-1304-0>.
- Sun, Y. Y., Gulizia, S., Oh, C. H., Doblin, C., Yang, Y. F., & Qian, M. (2015). Manipulation and characterization of a novel titanium powder precursor for additive manufacturing applications. *Jom Journal of the Minerals Metals and Materials Society*, 67(3), 564–572. Retrieved from <https://doi.org/10.1007/s11837-015-1301-3>.
- Sutton, A. T., Kriewall, C. S., Karnati, S., Leu, M. C., & Newkirk, J. W. (2020). Characterization of AISI 304L stainless steel powder recycled in the laser powder-bed fusion process. *Additive Manufacturing*, 32, 100981. Retrieved from <https://doi.org/10.1016/j.addma.2019.100981>.
- Trpělková, Ž., Hurychová, H., Kuentz, M., Vraníková, B., & Šklubalová, Z. (2020). Introduction of the energy to break an avalanche as a promising parameter for powder flowability prediction. *Powder Technology*, 375, 33–41. Retrieved from <https://doi.org/10.1016/j.powtec.2020.07.095>.
- Vock, S., Klöden, B., Kirchner, A., Weißgärber, T., & Kieback, B. (2019). Powders for powder bed fusion: A review. *Progress in Additive Manufacturing*, 4(4), 383–397. Retrieved from <https://doi.org/10.1007/s40964-019-00078-6>.

Appendix

Table A1. Measurement means and standard deviations from the RPA, in mJ/kg, degrees and g/cm³.

| | AE | AE, 15 RPM | BE | BE, 15 RPM | AA | AA, 15 RPM | Density |
|------|----------|---------------|----------|------------|----------|---------------|-----------|
| VIGA | 8.5±4.2 | 14.3±4.0 | 28.2±3.4 | 38±3.7 | 37.9±2.1 | 34.4±8.4 | 4.16±0.02 |
| GA | 13.1±4.4 | 12.1±3.8 | 28.7±3.2 | 37.5±2.2 | 34.6±1.8 | 33.4±6.1 | 4.17±0.03 |
| WA | 11±5.6 | 9.8±3.5 | 44.3±4.9 | 54.4±2.9 | 44.3±2.0 | 39.8±8.2 | 2.53±0.01 |
| WA-M | 8.7±4.1 | 14.4±5.4 | 30.9±3.3 | 44.1±4.2 | 38.2±1.7 | 36.2±8.0 | 3.62±0.01 |

Values are taken from both, flowability and multflow measurements (at 15 RPM).

Table A2. *t*-Tests of the RPA results of the VIGA and GA powder grades.

| | VIGA | GA | <i>t</i> -Test |
|------------|----------|----------|------------------|
| AE | 8.5±4.2 | 13.1±4.4 | <0.001 |
| AE, 15 RPM | 14.3±4.0 | 12.1±3.8 | <0.001 |
| BE | 28.2±3.4 | 28.7±3.2 | 0.223 |
| BE, 15 RPM | 38±3.7 | 37.5±2.2 | 0.041 |
| AA | 37.9±2.1 | 34.6±1.8 | <0.001 |
| AA, 15 RPM | 34.4±8.4 | 33.4±6.1 | 0.091 |

Bold values indicate that the difference is statistically significant.

Table A3. One-way ANOVA analysis of the porosity of printed specimens.

| | VIGA | GA | WA | WA-M | <i>F</i> -test |
|----------------|--------------|--------------|--------------|------------------|------------------|
| 20 μm | 0.03±0.01 | 0.05±0.01 | 0.03±0.01 | 0.06±0.03 | 0.311 |
| 40 μm | 0.03±0.01 | 0.06±0.01 | 1.77±0.93 | 0.20±0.04 | 0.014 |
| 60 μm | 0.07±0.01 | 0.08±0.01 | 3.91±1.04 | 0.70±0.28 | <0.001 |
| 80 μm | 0.06±0.02 | 0.16±0.05 | 4.86±1.99 | 3.93±0.76 | 0.005 |
| <i>F</i> -test | 0.003 | 0.011 | 0.017 | <0.001 | – |

Bold *F*-tests indicate that the difference is statistically significant.